PHCbi

70% of surveyed scientists admitted that they could not replicate someone else's research.[1]

50% admitted that they couldn't replicate their own research.[1]

Stability, Reproducibility and Accuracy

The complete selection of PHCbi brand CO_2 and multigas incubators includes benchtop, stackable and reach-in models to meet a wide range of culture conditions, space needs and decontamination method preferences.

- Standard inCu-saFe® copper enriched germicidal surfaces prevent contamination before it starts
- Select models feature integrated dual high heat or H_2O_2 vapor and SafeCell™ UV scrubbing which combine to increase *in vitro* cell safety

We have an incubator that will meet your needs. Visit our overview, "Choosing Your Cell Culture Incubator" to help make your selection.

PHC Corporation of North America

PHC Corporation of North America
1300 Michael Drive, Suite A, Wood Dale, IL 60191
Toll Free USA (800) 858-8442, Fax (630) 238-0074
www.phchd.com/us/biomedical

1) Baker, Monya. "1,500 scientists lift the lid on reproducibility." Nature, no. 533 (May 26, 2016): 452-54. doi:10.1038/533452a.

Received: 28 August 2019 | Revised: 6 November 2019 | Accepted: 10 November 2019

DOI: 10.1002/bit.27226

ARTICLE

BIOTECHNOLOGY BIOENGINEERING WILEY

Targeted delivery of functionalized PLGA nanoparticles to macrophages by complexation with the yeast *Saccharomyces cerevisiae*

Ruth Kiefer[1] | Marijas Jurisic[2] | Charlotte Dahlem[3] | Marcus Koch[4] | Manfred J. Schmitt[1] | Alexandra K. Kiemer[3] | Marc Schneider[2] | Frank Breinig[1]

[1]Molecular and Cell Biology, Saarland University, Saarbrücken, Germany

[2]Department of Pharmacy, Biopharmaceutics and Pharmaceutical Technology, Saarland University, Saarbrücken, Germany

[3]Department of Pharmacy, Pharmaceutical Biology, Saarland University, Saarbrücken, Germany

[4]INM - Leibniz -Institute for New Materials, Saarbrücken, Germany

Correspondence
Frank Breinig, Molecular and Cell Biology, Building A1.5, Saarland University, D-66123 Saarbrücken, Germany.
Email: fb@microbiol.uni-sb.de

Funding information
Saarland Landesforschungsförderung, Grant/Award Numbers: LFFP 1303, LFFP 17/08; Deutsche Forschungsgemeinschaft, Grant/Award Number: KI702

Abstract

Nanoparticles (NPs) are able to deliver a variety of substances into eukaryotic cells. However, their usage is often hampered by a lack of specificity, leading to the undesired uptake of NPs by virtually all cell types. In contrast to this, yeast is known to be specifically taken up into immune cells after entering the body. Therefore, we investigated the interaction of biodegradable surface-modified poly(lactic-*co*-glycolic acid) (PLGA) particles with yeast cells to overcome the unspecificity of the particulate carriers. Cells of different *Saccharomyces cerevisiae* strains were characterized regarding their interaction with PLGA-NPs under isotonic and hypotonic conditions. The particles were shown to efficiently interact with yeast cells leading to stable NP/yeast-complexes allowing to associate or even internalize compounds. Notably, applying those complexes to a coculture model of HeLa cells and macrophages, the macrophages were specifically targeted. This novel nano-in-micro carrier system suggests itself as a promising tool for the delivery of biologically active agents into phagocytic cells combining specificity and efficiency.

KEYWORDS
drug delivery, immunotherapy, nanomedicine, phagocytosis, yeast

1 | INTRODUCTION

Delivery of biologically active agents to specific cells or tissues represents a promising therapeutic approach. However, effective targeting of particular cell types still remains a significant challenge with major obstacles. In the field of nonviral carrier systems, nanoparticles (NPs) have been extensively studied as a vehicle for immunotherapy (Amoozgar & Goldberg, 2015). Among the enormous amount of different NP compositions described so far, biocompatible polymers possess several advantages with regard to stability, safety, or controlled-release ability. Likewise, their high variability in size and charge makes them a very interesting carrier system for drugs, nucleic acids, or other biologically active agents (Bala, Hariharan, & Kumar, 2004; Nafee, Taetz, Schneider, Schaefer, & Lehr, 2007). The biodegradable and biocompatible poly(lactic-*co*-glycolic acid) (PLGA), already being approved as generally recognized as safe (GRAS) from the Food and Drug Administration (FDA) and European Medicine Agency (EMA; Mir, Ahmed, & Rehman, 2017), represents one of the most promising materials. Additionally, PLGA-NPs stand out from their high cargo capacity, ease of production and modification, as well as the ability to escape from early endosomes into the cytoplasm (Hamdy, Haddadi, Hung,

& Lavasanifar, 2011). However, even though both uptake and retention of nanoparticles in target cells can be enhanced by modifying the surface with particular ligands or varying their physicochemical properties, there is still a need for improvement to eliminate off-target accumulation and uptake by undesired cell types (Brown, Pistiner, Adjei, & Sharma, 2019).

Macrophages are specialized cells involved in a variety of immunological mechanisms comprising, amongst others, phagocytic clearance, antigen processing and presentation, inflammatory or anti-inflammatory regulation, and tissue repair. This broad spectrum of functions requires high phenotypic plasticity that is enabled by a highly variable transcriptional repertoire responding to different microenvironmental signals (Mosser & Edwards, 2008; Reinartz et al., 2014). In fact, macrophages can undergo a spectrum of activation states, wherein M1 and M2 represent two extremes (Biswas & Mantovani, 2010; Verreck, de Boer, Langenberg, van der Zanden, & Ottenhoff, 2006; Xue et al., 2014). Besides pathogen clearing and activation of the adaptive immune response, M1 macrophages are also involved in chronic inflammatory diseases and tumor repression, whereas the M2 subtype behaves immunosuppressive and promotes tumor growth (Murray & Wynn, 2011). Accordingly, the re-education of macrophages represents a very promising strategy in different therapeutic approaches for cancer or arthritis, and several substances with reprogramming effects have already been described (Jain, Tran, & Amiji, 2015; Rubio et al., 2019; Wang et al., 2017). Amongst others, imiquimod, interferon-γ (IFN-γ), and interleukin-12 (IL-12) have been demonstrated to exert an antitumor function, but would lead to severe off-target effects after systemic administration (Dewan et al., 2012; Dunn, Koebel, & Schreiber, 2006; Wang et al., 2017). Thus, to avoid such negative side effects, there is a strong need for an effective and safe cell-specific delivery system.

Yeast cells have been repeatedly proven to be a remarkably efficient delivery vehicle for targeting a whole bunch of cargos to phagocytic cells in general and macrophages in particular (Bazan, Geginat, Breinig, Schmitt, & Breinig, 2011; Seif, Hoppstädter, Breinig, & Kiemer, 2017; Seif, Philippi, Breinig, Kiemer, & Hoppstadter, 2016; Stubbs et al., 2001; Walch, Breinig, Schmitt, & Breinig, 2012). Among the different yeast genera, the well-characterized baker's yeast *Saccharomyces cerevisiae* possesses the GRAS status facilitating a possible application as a carrier system, thereby providing the advantages of a single cell organism including easy handling and genetic modification. In addition, *S. cerevisiae* harbors the opportunity of oral delivery as it is able to protect a cargo from degradation by acidic pH or proteases during gastrointestinal passage and is efficiently taken up by specialized M cells in the gut (Beier & Gebert, 1998; Kenngott et al., 2016). Furthermore, glucan particles, derived from the cell wall of *S. cerevisiae*, have already been successfully examined for oral as well as systemic delivery of NPs to macrophages (Soto, Caras, Kut, Castle, & Ostroff, 2012; Soto & Ostroff, 2008). In addition, positively charged nanoparticles could be effectively loaded into yeast capsules by electrostatic forces-mediated spontaneous deposition (Ren et al., 2018; Zhou et al., 2017).

In this study, we aimed to establish a completely GRAS nano-in-micro delivery system for macrophages by combining the advantages of yeast cells and PLGA-NPs. We show that PLGA-NPs strongly interact with yeast cells and the generated yeast/NP complexes are targeted specifically to macrophages with high efficiency. This system raises the possibility to deliver a variety of biologically functional agents to macrophages for being used in therapeutic approaches.

2 | MATERIALS AND METHODS

2.1 | Yeast strains and cell culture

S. cerevisiae strains S86c [MATα *ura3-2 leu2 his3 pra1 prb2 prc1 cps1*] and BY4742 [MATα *his3Δ1 leu2Δ0 lys2Δ0 ura3Δ0*] were grown in YPD (1% yeast extract, 2% peptone, 2% glucose) at 30°C and 220 rpm. For fluorescence labeling, 10^7 yeast cells were harvested by centrifugation (14,000×*g*, 5 min), washed with phosphate-buffered saline (PBS; Biochrom, Berlin, Germany), and stained with 2.5 μM carboxyfluorescein diacetate succinimidyl ester (CFSE; Life Technologies, Carlsbad, CA) for 30 min at 37°C. CFSE-stained yeast cells were washed twice with PBS to remove the residual dye and opsonized by incubation with 25% human serum for 30 min at 37°C.

The human cervix tumor cell line HeLa was cultured in Roswell Park Memorial Institute 1640 (RPMI-1640) supplemented with 10% fetal bovine serum (FBS) (Sigma-Aldrich, St. Louis, MO), 100 U/ml penicillin, 100 mg/ml streptomycin, and 2 mM glutamine. Cells were cultivated in a humidified atmosphere with 5% CO_2 at 37°C and passaged twice a week. The human monocyte cell line THP-1 (ATCC® TIB-202™) was cultured in RPMI-1640 medium (Sigma-Aldrich) supplemented with 10% FBS; Biochrom). Cells were grown in a humidified 5% CO_2 atmosphere at 37°C. Monocytes were differentiated into M1 or M2 macrophages as previously described by adding 30 ng/ml phorbol 12-myristate-13-acetate (PMA; Sigma-Aldrich; Hoppstädter et al., 2015; Kiemer et al., 2009). After 48 hr, cells were stimulated for another 40 hr with 1 μg/ml LPS (Sigma-Aldrich) and 20 ng/ml recombinant human IFN-γ or 200 ng/ml recombinant human IL-10 (both from Miltenyi Biotec, Bergisch Gladbach, Germany), respectively.

2.2 | Isolation and culture of primary human monocyte-derived macrophages

The isolation of primary cells from human material was authorized by the local ethics committee (State Medical Board of Registration, Saarland, Germany; permission no. 173/18). Human monocytes were isolated from buffy coats obtained from anonymous healthy blood donors (Blood Donation Center, Saarbrücken, Germany). Peripheral blood mononuclear cells (PBMC) were separated by density gradient centrifugation using Lymphocyte Separation Medium 1077 (PromoCell, Heidelberg, Germany) in Leucosep tubes (Greiner Bio-One, Kremsmünster, Austria). PBMC were washed in PBS and monocytes were separated by positive selection using magnetic anti-CD14 microbeads (Miltenyi Biotec). For macrophage differentiation, monocytes were cultured at a density of 1.5×10^7 cells per 175 cm^2 flask in

RPMI-1640 medium supplemented as above and 20 ng/ml human recombinant macrophage colony-stimulating factor (M-CSF; Miltenyi Biotec) for 5 days, as described previously (Seif, Philippi, Breinig, Kiemer, & Hoppstädter, 2016). Macrophages were maintained at 37°C in a humidified atmosphere of 5% CO_2, and the medium was changed every second day.

2.3 | Nanoparticles

The nanoparticles were prepared using the solvent-diffusion evaporation technique as similar to Nafee et al. (2007) in a one-pot approach. In brief, 50 mg of rhodamine-labeled PLGA (prepared as described by Lababidi et al., 2019) were dissolved in 4.5 ml ethyl acetate (Thermo Fisher Scientific, Schwerte, Germany). In parallel 7.5 ml of an aqueous 2% polyvinyl alcohol (PVA; Mowiol 4-88, Kuraray Europe, Hattersheim, Germany) solution containing 22 mg of chitosan (Protasan UP CL 113, NovaMatrix, Dupont, Sandvika, Norway) was prepared. Afterward, the two solutions were mixed with each other using an ultrasound device (MS73 head, Sonoplus HD 3100, Bandelin electronic GmbH & Co. KG, Berlin, Germany) at 30% amplitude for 30 s. Then to obtain the hypotonic particle solution, 45 ml of MiliQ water (Merck Millipore, Darmstadt, Germany) was added and the mixture was left overnight under stirring to remove the organic solvent.

To obtain the particles dispersed at nearly isotonic conditions, 67 mg NaCl (Carl Roth, Karlsruhe, Germany) was added to the 2% PVA solution (with or without chitosan) before combining with the PLGA containing phase. After particle formation, the volume was increased by adding 45 ml of 0.9% NaCl. Colloidal properties of the particles were determined with a Zetasizer Nano (Malvern, Malvern, UK) and are displayed in Table 1 indicating the sizes and the small size distributions.

2.4 | Yeast–nanoparticle interaction

For interaction studies, 10^7 yeast cells were harvested by centrifugation (14,000 ×*g*, 5 min), resuspended in 100 µl of the corresponding nanoparticle solution (0.03–1 mg/ml in isotonic [154 mM] as well as hypotonic [5 mM] NaCl solution) and incubated for 1 hr at 20°C with gentle shaking. Afterward, the yeast/NP suspension was diluted with sterile H_2O resp. PBS, layered over 13% sucrose, and centrifuged at 600 × *g* in a swing bucket rotor for 10 min without brake to separate unbound particles from yeast cells, if needed. For analysis of membrane integrity, yeast cells were stained with propidium iodide (PI) for 5 min (final concentration 5 µg/ml). After washing with PBS, 30,000 cells were analyzed via flow cytometry on a BD LSRFortessa™ using the FACSDiva™ software (BD Biosciences, Franklin Lakes, NJ). To further characterize the yeast/NP interaction, yeast cells were stained with Concanavalin A CF™488 A (50 µg/ml, Biotium, Freemont, CA) for 30 min at RT. After washing with PBS, stained yeast cells were incubated with NPs as described above. The resulting solution was mixed at a ratio of 3:2 with FluorSave™ reagent (Calbiochem®), spotted on a slide, and topped with a coverglass. After approximately 1 hr, the sample was examined using a Zeiss Axio Observer with an LSM 710 Scanning Module and ZEN 2 (blue edition) software (Zeiss, Jena, Germany).

TABLE 1 Physicochemical characteristics of chitosan-coated nanoparticles in 5 and 154 mM NaCl solution ($n = 3$, mean ± *SD*)

	NaCl	
	5 mM	154 mM
Size (nm)	237.5 ± 3.2	202.3 ± 2.7
PDI	0.09 ± 0.018	0.046 ± 0.006
ζ-Potential (mV)	11.6 ± 1.4	3.25 ± 0.3
Conductivity (mS/cm)	0.516 ± 0.014	19.4 ± 1.7
pH	3.97 ± 0.3	3.9 ± 0.2

2.4.1 | Electron microscopy

For transmission electron microscopy (TEM) a droplet of the respective solution was placed onto a holey carbon TEM grid (type S147-4; Plano, Wetzlar, Germany) and dried at ambient conditions. TEM analysis was performed using a Jeol (Akishima, Tokio, Japan) JEM-2100 LaB6 transmission electron microscope operating at 200 kV accelerating voltage. A Gatan (Pleasanton, CA) Orius SC1000 CCD camera was used to get TEM bright-field images with 1024 × 1024 pixels (binning 2, acquisition time 0.5 s).

For scanning electron microscopic (SEM) imaging a droplet of the sample solution was rinsed over a holey carbon grid (type S 147-4; Plano, Wetzlar, Germany), dried at air and fixed to the SEM sample holder using double-sided carbon tape. A thin layer of gold-palladium (ratio 60:40) was deposited onto the samples using magnetron sputter deposition (Jeol JFC-1300, 20 mA, 30 s). Secondary electron imaging was performed using an FEI Quanta 400 FEG under high vacuum conditions at 20 kV accelerating voltage.

2.5 | Uptake of yeast/NP complexes by macrophages

2.5×10^5 cells/ml THP-1 monocytes were seeded into 35 mm dishes (ibidi, Martinsried, Germany), polarized into M1 and M2 MΦ as described above and incubated with NP-complexed yeast cells at a multiplicity of infection (MOI) of 5 or 50 µg/ml NPs for 16 hr at 37°C and 5% CO_2. After two washing steps with PBS, cells were stained with CellMask™ Green (Life Technologies) for 5 min at 37°C, fixed with 4% formaldehyde and counter-stained with 4′,6-diamidino-2-phenylindole (DAPI). Finally, macrophages were covered with phenol red-free RPMI-1640 and analyzed with a Zeiss Axio Observer and LSM 710 Scanning Module (Zeiss, Jena, Germany). Z-stack images were collected in 1 µm sections and presented as an orthogonal view using ZEN 2 (blue edition) software (Zeiss).

For additional quantitative analyses, THP-1 monocytes were seeded at a density of 2.5×10^5 cells/ml in 24-well plates,

differentiated into macrophages and treated with yeast/NP complexes as described above. Subsequently, macrophages were washed two times with PBS and detached using a cell scraper. After centrifugation (300 ×*g*, 10 min) cells were resuspended in 1% formaldehyde and 10,000 macrophages were examined on a BD LSRFortessa™ using BD FACSDiva™ software (BD Biosciences).

2.6 | Coculture and uptake studies

Primary monocyte-derived macrophages (MDM) were isolated and differentiated as described above. On Day 5, macrophages were harvested using accutase solution (Sigma) and stained with cell tracker deep red dye (Thermo Fisher Scientific) in a working concentration of 500 nM dissolved in RPMI-1640 for 30 min at culturing conditions. HeLa cells were harvested by trypsin detachment and stained with 5 μM cell tracker violet BMQC (Thermo Fisher Scientific) for 30 min. Cells were washed twice with PBS and suspended in the culture medium. HeLa and macrophages were cultured in a 1:1 ratio (2.5×10^5 cells, each, seeded in six-well plates) for 24 hr. For uptake studies, free rhodamine-labeled nanoparticles (NPs) or NPs complexed to CFSE-stained yeast (as described above) were added to the coculture at 37°C in 5% CO_2 for 0.5 or 4 hr. Yeast cells were added at a MOI of 5, and plain NPs in the corresponding amount that was loaded to yeast (which equals 38 μg). Plates were briefly centrifuged to ensure that yeast and the cell coculture were in close contact. After incubation, supernatants were collected, and cells were harvested using PBS containing 5 mM ethylenediaminetetraacetic acid. Supernatants together with harvested cells were centrifuged, resuspended in 1% formaldehyde in PBS, and examined via flow cytometry as described above. A small fraction of analyzed cells (4.2% ± 2.1 *SD*) were cell tracker deep red and violet double positive. We suggest that this occurred from the engulfment of HeLa cell debris by macrophages. These cells were excluded from further analysis to allow a cell type-specific examination of NP uptake.

2.7 | Determination of cell viability

The 3-(4,5-dimethyl-thiazol-2-)-2,5-diphenyl tetrazolium bromide (MTT) colorimetric assay was used to analyze the toxic effect of NPs on yeast cells. After incubation with the indicated NP solution, yeast cells were washed with YPD and supplemented with 100 μg/ml MTT for 2 hr at 30°C. Cells were then solubilized using dimethyl sulfoxide and absorption was measured at 550 nm in a microplate reader SpectraMax® Paradigm® Multi-Mode Microplate Platform using Multi-Mode Analysis Software (Molecular devices). To analyze the effect of yeast/NP complexes on the viability of macrophages, THP-1 monocytes were differentiated into macrophages by adding 30 ng/ml PMA for 48 hr. Macrophages were cocultured overnight with yeast cells or yeast/NP complexes (MOI 5) and harvested using PBS. Cells were then stained with 2 μg/ml PI on PBS for 10 min at 4°C. After washing with PBS, 10,000 cells were analyzed via flow cytometry on a BD LSRFortessa™ using the FACSDiva™ software (BD Biosciences, Franklin Lakes, NJ).

3 | RESULTS

3.1 | Interaction of yeast cells with chitosan-coated PLGA particles

The ability of yeast cells to transport proteins, nucleic acids, or other biologically active agents into mammalian phagocytic cells has been shown repeatedly (Bazan, Breinig, Schmitt, & Breinig, 2014; Bazan et al., 2011; Seif, Hoppstädter, Breinig, & Kiemer, 2017; Walch, Breinig, Geginat, Schmitt, & Breinig, 2011; Walch-Rückheim, Kiefer, Geginat, Schmitt, & Breinig, 2016). To extend the described variety of applications, we investigated the capability of *S. cerevisiae* to associate with chitosan-coated PLGA nanoparticles to target the NPs specifically to phagocytes. Therefore, cells of two *S. cerevisiae* strains (BY4742 and S86c) were incubated with NPs at different concentrations ranging from 0.03 to 1 mg/ml. In preliminary experiments, the zeta potential of both strains was determined: based on their particular cell wall composition, the strains were found to differ in surface charge (−16 mV for BY4742 and −11 mV for S86c) and, thus, might interact differently with the NPs. Additionally, as the NaCl concentration was found to possess a major impact on the interaction between positively charged nanoparticles and yeast cells (Nomura et al., 2013), we studied and characterized the yeast-NP association in both isotonic (154 mM) as well as hypotonic NaCl solution (5 mM).

After incubation with the respective rhodamine-tagged NP solution under hypotonic conditions, flow cytometric analyses revealed very high amounts of yeast cells positive for particle-associated fluorescence as expected due to a lower shielding of the charge. The particle-associated fluorescence was ranging from 86% to almost 100% overall NP concentrations apart from the lowest (Figure 1a). In contrast, isotonic conditions not only yielded clearly less NP-positive yeast cells with a maximum of 68% at the highest NP concentration but also a slower increase in the amount of rhodamine-positive yeast cells towards higher concentrations.

Regarding the mean fluorescence intensities reflecting the number of interacting NPs, the influence of the NaCl concentration becomes even more distinct (Figure 1b) with a maximum intensity of 1,000 for isotonic and up to 13,000 (BY4742) and 10,000 (S86c), respectively, for hypotonic salt concentrations. Remarkably, under low-salt conditions, fluorescence intensity peaks reliably at a concentration of 0.25 mg/ml. These data indicate that both *S. cerevisiae* strains are able to interact effectively with chitosan-coated NP, especially under hypotonic conditions, with a slight bias regarding the interaction strength towards BY4742. Additionally, scanning electron microscopy (SEM) of chitosan-coated PLGA NP and the respective yeast/NP complexes proved the interaction of yeast cells and NPs (Figure 2).

Based on these results, we investigated by confocal fluorescence microscopy if NPs simply bind to yeast cells or even become internalized (CLSM; Figure 3). Therefore, cells of both yeast strains were exposed to rhodamine-tagged NPs under hypotonic conditions using concentrations of 0.25 and 1 mg/ml. Additionally, the yeast cell

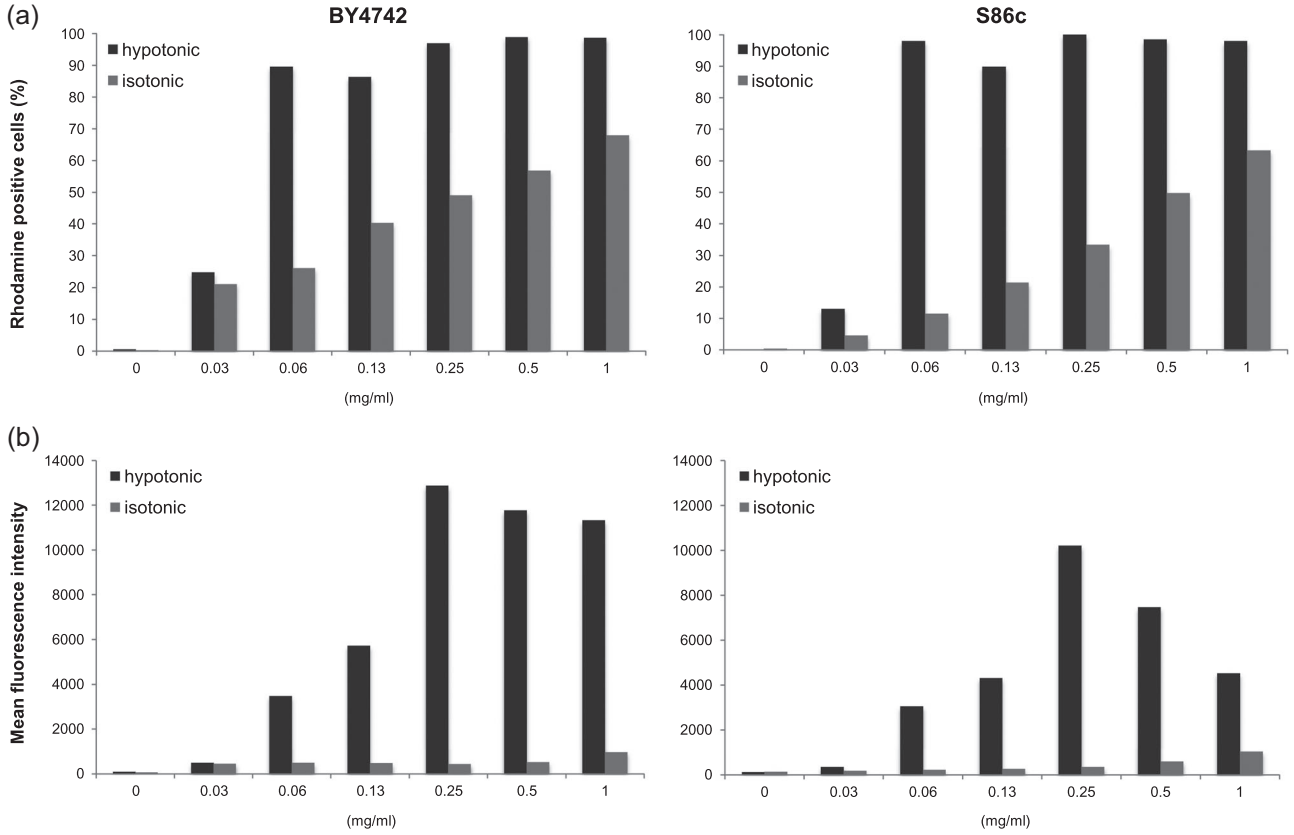

FIGURE 1 Interaction of two different *Saccharomyces cerevisiae* strains with rhodamine-tagged chitosan-coated poly(lactic-*co*-glycolic acid) (PLGA) particles. Yeast cells were incubated in 100 µl of the respective nanoparticle solution for 1 hr at 20°C. Rhodamine fluorescence was analyzed by flow cytometry. Data in the top row (a) represent the percentage of rhodamine-positive yeast cells of the strains BY4742 (left) and S86c (right). Corresponding mean fluorescence intensities are displayed in the bottom row (b)

wall was stained with ConA-488 allowing a better visualization of particle adhesion and/or internalization in relation to the cell surface. Whereas the control cells without NPs showed only green fluorescent cell walls, addition of NPs at high concentration led to a distribution of red fluorescence all over the yeast cells in both strains, again with a higher signal intensity for BY4742 (cf. Figures 3a and 3b). Fluorescence intensity profiles of representative cells confirm these observations indicating both, particle binding to the cell wall as well as internalization by the yeast cells under these conditions. On the other hand, lower NP concentration led to a pronounced particle accumulation at the cell wall in BY4742 and, although to a lesser extent, also in S86c as likewise approved by the colocalization of green and red fluorescence within the respective cells. As already depicted in Figure 1b the rhodamine fluorescence intensities of yeast cells incubated with NPs under isotonic conditions are very low compared with hypotonic conditions and, thus, a possible interaction between yeast cells and NPs could not be visualized via CLSM in isotonic salt concentrations. Taken together,

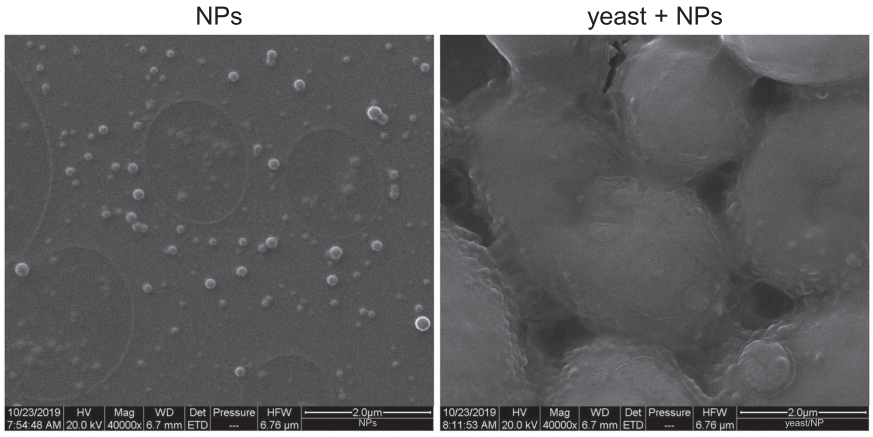

FIGURE 2 Distribution of NPs on the yeast cell surface. Yeast cells of the strain BY4742 were incubated with 1 mg/ml NPs (5 mM NaCl) for 1 hr and examined via SEM. Representative images of both, the original nanoparticle solution (left), and yeast/NP complexes (right) are shown. NP, nanoparticle; SEM, scanning electron microscopy

interactions of both analyzed *S. cerevisiae* strains with chitosan-coated NPs could be demonstrated. Due to the fact, that our data suggest a somewhat higher NP-binding efficiency in BY4742, we focused on this strain in all further experiments.

3.2 | Effect of chitosan-coated PLGA particles on yeast cells

The observed strong interaction of yeast cells with NPs rose the question if binding of the particles to or internalization by the yeast

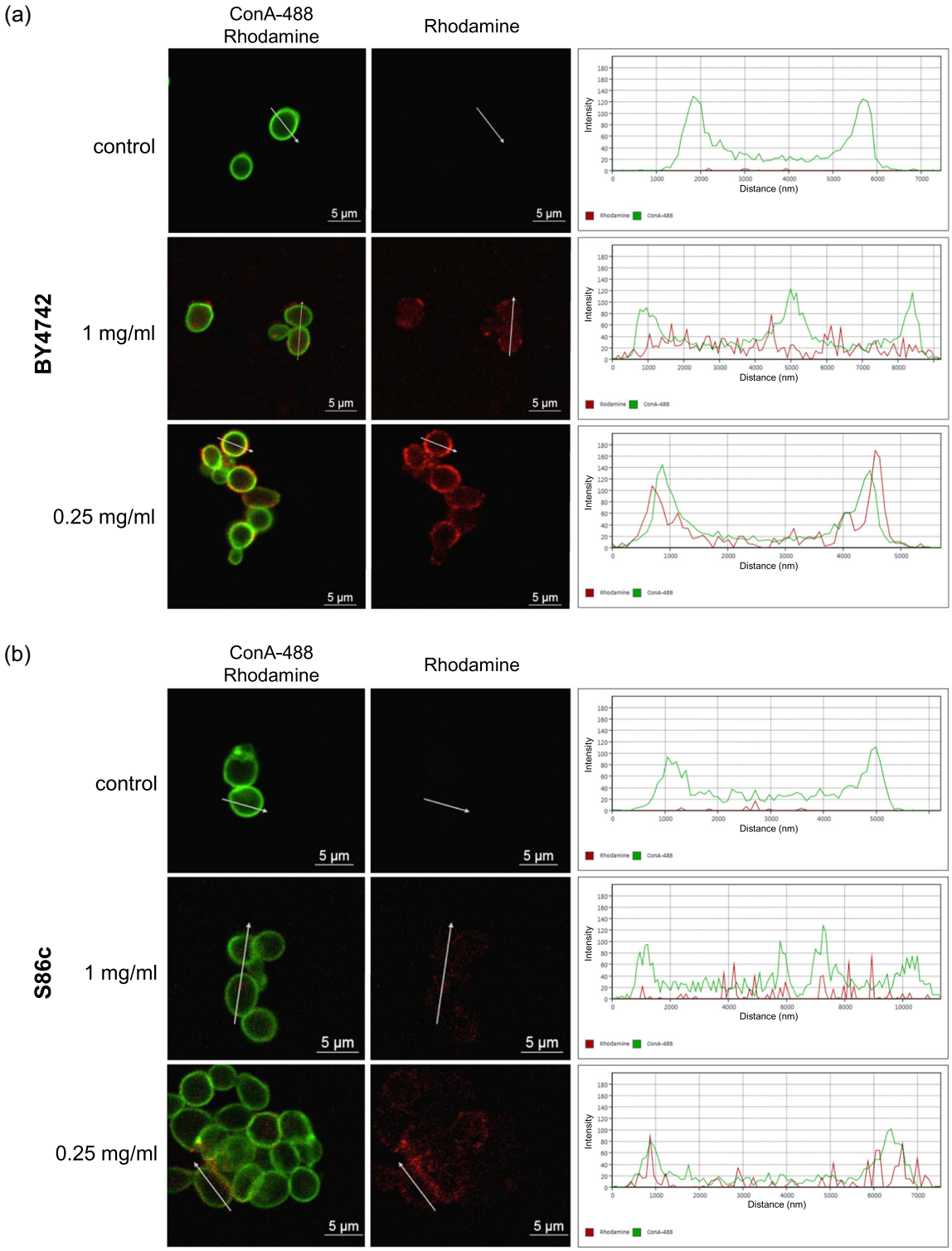

FIGURE 3 CLSM images of yeast cells after incubation with rhodamine-tagged PLGA particles. Displayed are yeast cells of the strains BY4742 (a) and S86c (b) incubated with 1 and 0.25 mg/ml NP solution (5 mM NaCl) or water for the control. Yeast cell walls were stained with ConA-488. In the right column, one representative fluorescence intensity profile is shown for each sample. CLSM, confocal laser scanning microscopy; NP, nanoparticle; PLGA, poly(lactic-*co*-glycolic acid) [Color figure can be viewed at wileyonlinelibrary.com]

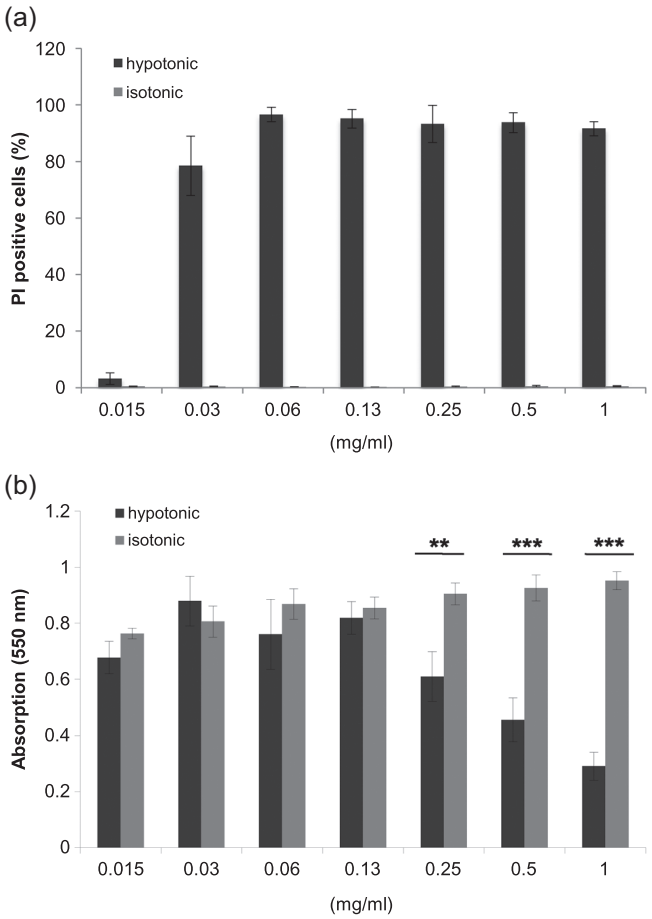

FIGURE 4 Influence of PLGA-NPs on membrane integrity and viability of *Saccharomyces cerevisiae* BY4742. Yeast cells were incubated with different concentrations of NPs dispersed in either 5 mM or 154 mM NaCl solution. (a) Cells were stained with propidium iodide and analyzed via flow cytometry. Data are presented as percentage of PI-positive cells ± *SD* of three independent samples. (b) Viability of yeast cells based on an MTT assay. Data represent the absorption means ± *SD* of four independent samples. MTT, 3-(4,5-dimethyl-thiazol-2-)-2,5-diphenyl tetrazolium bromide; NP, nanoparticle; PI, propidium iodide; PLGA, poly(lactic-*co*-glycolic acid). *p* values were generated by Student's *t* test (**$p < .005$, ***$p < .001$)

cells affects membrane integrity and, eventually, cell viability. As membrane integrity can be verified by PI staining, BY4742 cells were incubated for 1 hr with different amounts of untagged NPs (i.e. without rhodamine) and PI-positive cells were quantified by FACS analyses. Under hypotonic conditions, about 90% of the yeast cells were PI-positive over a wide range of NP concentrations, clearly indicating the formation of pores in the yeast cell membrane (Figure 4a). In sharp contrast, under isotonic conditions, virtually no PI-positive cells could be detected. However, as the impairment of membrane integrity is not necessarily associated with a decreased viability, we performed MTT assays to test the actual viability of yeast cells (Figure 4b). In direct comparison with the isotonic setting, yeast viability evidently correlated with NP concentrations with a significant reduction above 0.25 mg/ml NPs under hypotonic conditions, reducing survival to 30% at the highest concentration. At lower NP concentrations, no significant difference between low and high salt incubation could be detected. Comparable results were obtained in corresponding plate assays (not shown). In sum, these findings imply that chitosan-coated NPs weaken membrane integrity of yeast cells under hypotonic but not under isotonic conditions. However, this interaction impairs the viability of yeast cells merely at high NP concentration.

3.3 | Uptake of yeast/NP complexes by macrophages

Recognition and subsequent uptake of the respective carrier by phagocytic cells is an important prerequisite for efficient delivery into these cells. Thus, we performed preliminary experiments to ensure effective phagocytosis of BY4742 cells by M1- and M2-polarized macrophages derived from human THP-1 monocytes. CFSE-stained yeast cells were opsonized with human serum or left untreated and

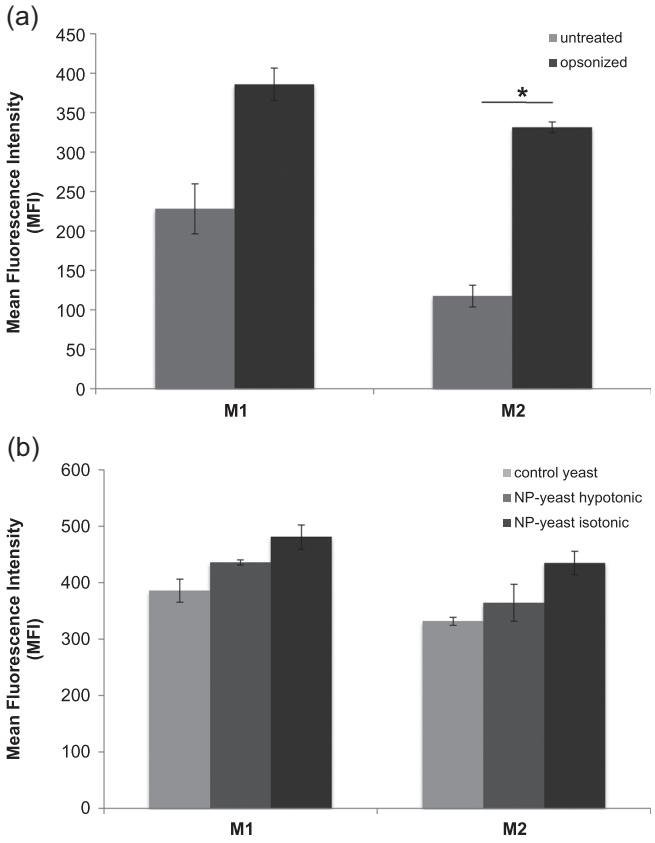

FIGURE 5 Uptake of *Saccharomyces cerevisiae* by M1- and M2-polarized THP-1 macrophages. MΦ were incubated with CFSE-stained yeast cells at MOI 5 for 4 hr. The mean fluorescence intensity of CFSE-positive macrophages was determined by flow cytometry. (a) Comparison of untreated and opsonized yeast cells. (b) Uptake of NP-loaded yeast in different NaCl concentrations compared with unloaded control cells. Experiments were performed in doublets. CFSE, carboxyfluorescein diacetate succinimidyl ester; MOI, multiplicity of infection; NP, nanoparticle. *p* Values were generated by Student's *t* test (*$p < .05$)

incubated with M1 or M2 macrophages at MOI 5; subsequently, macrophages that had taken up yeast cells were quantified via flow cytometry based on their CFSE-positive signal (Figure 5a). Although not fully statistically significant ($p = .07$) for M1, in either case, opsonized yeast cells showed a higher uptake rate than untreated yeast cells. This observation is in accordance with our previous data on the uptake of non-opsonized yeast cells by primary human macrophages (Seif et al., 2016). Accordingly, opsonized yeast was used for all further experiments. Since the recognition of yeast cells by macrophages is based on the interaction of specific receptors on the macrophages with their respective ligand within the yeast cell wall, we next investigated if the coating of yeast cells with NPs has any influence on this interaction. This is clearly not the case as yeast/NP complexes produced either under isotonic or hypotonic conditions did not show a reduced uptake, excluding any negative side effect of the NPs on the recognition or uptake of the yeast cells by the macrophages (Figure 5b). Interestingly, the yeast/NP complexes actually showed a slight tendency towards better uptake, especially in M2 macrophages. To rule out any negative effect of yeast/NP complexes on macrophages, a viability test was performed using PI staining. Therefore, BY4742 yeast cells were complexed with unlabeled NPs and cocultured with macrophages overnight at an MOI of 5. Compared to untreated control cells, there was no impairment of cell viability detectable (Figure S1).

Afterward, we tested the targeting of yeast/NP complexes to macrophages in comparison to a pure NP solution (50 µg/ml). Therefore, BY4742 yeast cells were preincubated with rhodamine-labeled NP solutions (1 mg/ml) under low/high salt conditions and separated from unbound particles *via* density gradient centrifugation indicating that approx. 62% of the NPs remained in the aqueous solution. The separation of free NPs was visualized via TEM (Figure S2). The received yeast/NP complexes were then cocultivated with prepolarized M1 and M2 macrophages at MOI 5 for 16 hr; untreated macrophages served as

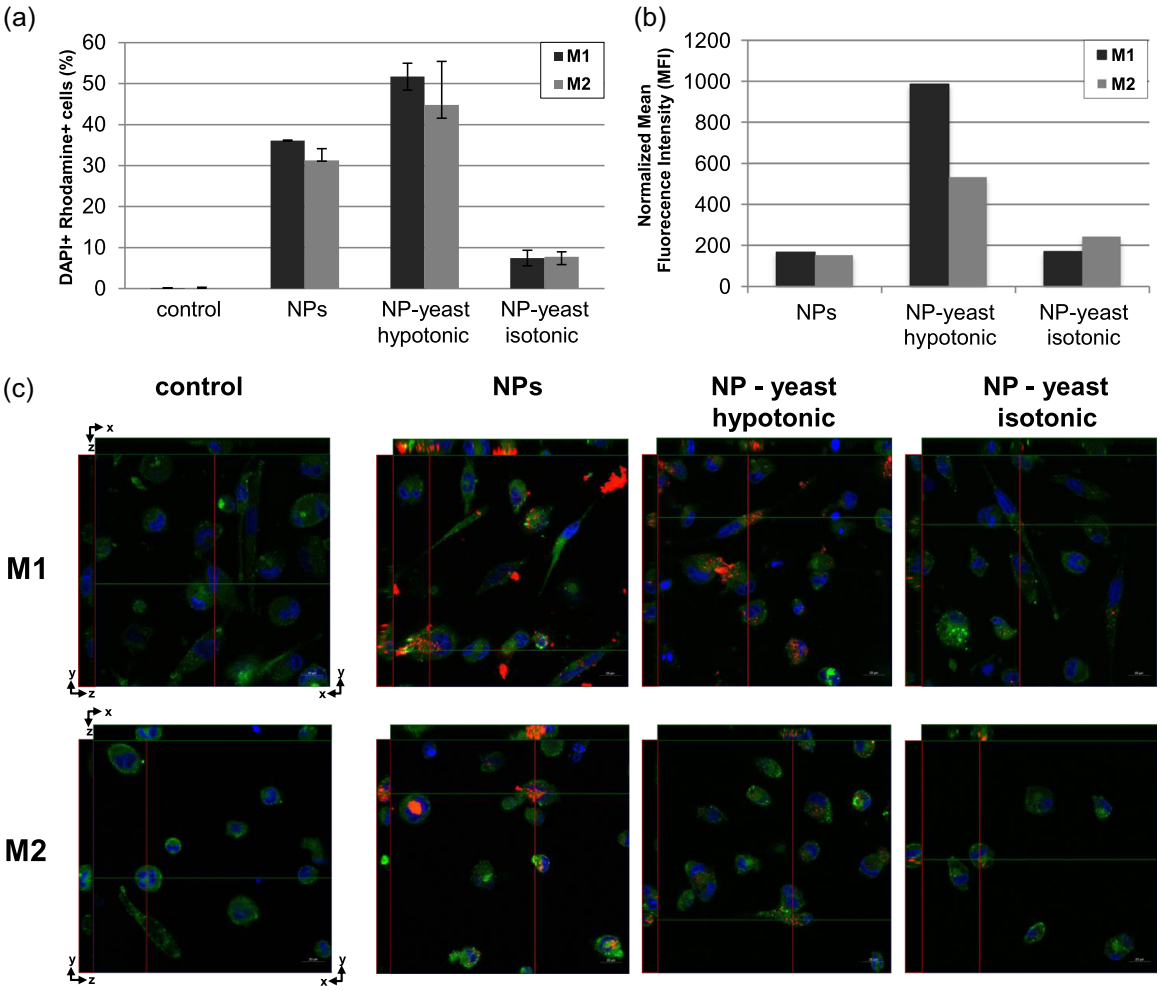

FIGURE 6 Delivery of rhodamine-tagged NPs to macrophages via yeast cells. M1 and M2 MΦ were incubated for 16 hr with NPs only or NP-complexed yeast cells and were stained with DAPI (nucleus, blue) and CellMask (cytosol, green). Yeast cells were preincubated with NPs dispersed in either 5 or 154 mM NaCl solution. (a) Quantitative analysis via flow cytometry; data represent the percentage of DAPI/rhodamine-positive MΦ ± *SD* of three independent samples. (b) Fluorescence intensity of M1 and M2 MΦ normalized to the applied amount of NPs. (c) Orthogonal view of CLSM images showing M1 (top row) and M2 MΦ (bottom row). The central image shows the horizontal (*x*–*y*) section; top and side panels represent the *x*–*z* and *y*–*z* planes, respectively. CLSM, confocal laser scanning microscopy; DAPI, 4′,6-diamidino-2-phenylindole; NP, nanoparticle [Color figure can be viewed at wileyonlinelibrary.com]

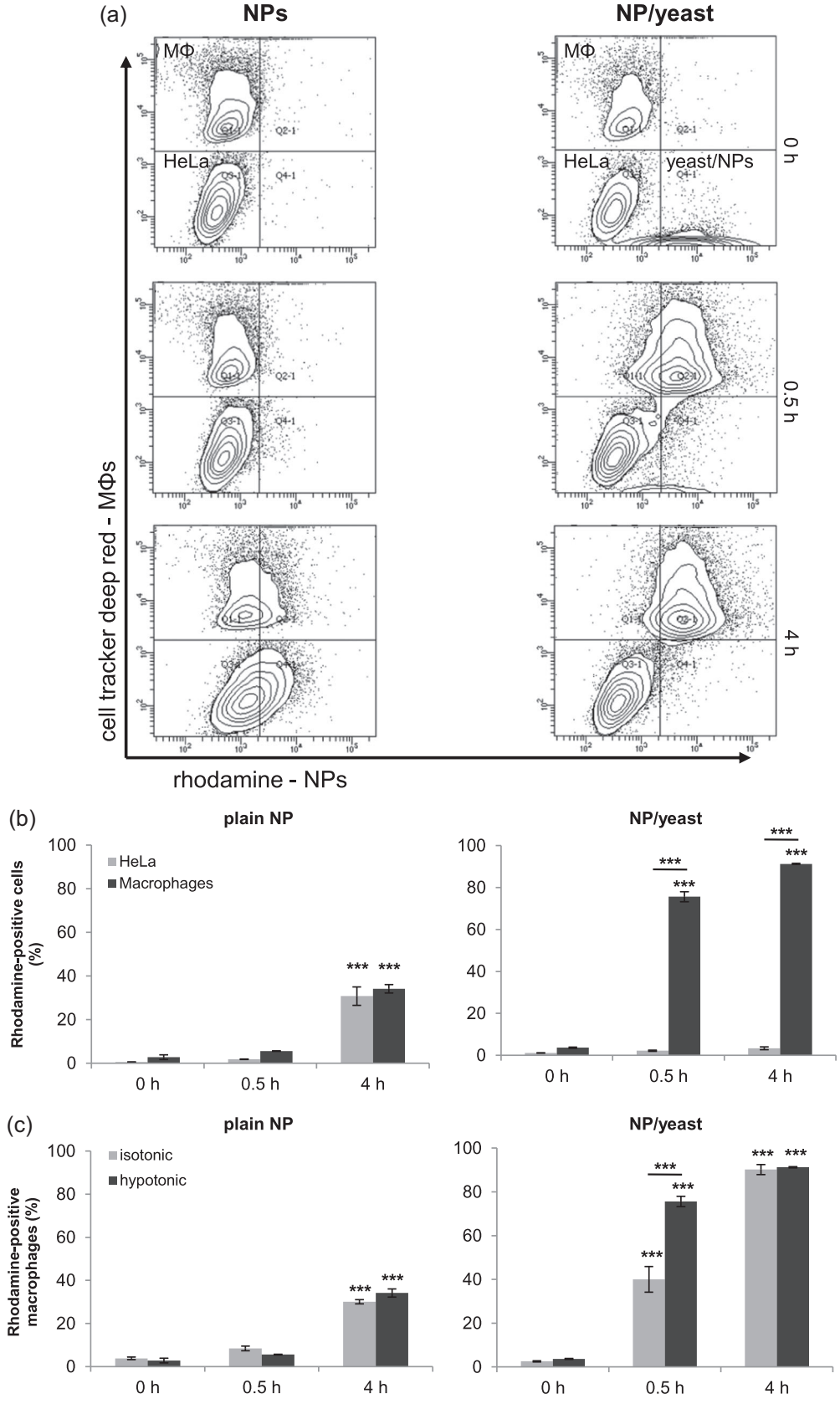

FIGURE 7 Continued.

a negative control. Subsequently, particle internalization with or without yeast cells was assessed via flow cytometry based on a DAPI (macrophages)/rhodamine (NPs) double fluorescence. In this setting, yeast/NP complexes produced under hypotonic conditions were taken up with the highest efficacy in both M1 and M2 macrophages compared with isotonic conditions, and, remarkably, also to the much higher concentrated pure NPs (Figure 6a). Among the subtypes, there was a bias to M1 in comparison to M2 macrophages for plain NPs as well as yeast/NP complexes under hypotonic conditions, respectively. The lowest particle-associated fluorescence was observed for yeast/NP complexes produced in isotonic solution with values clearly below 10% in either case, with a very slight bias to M2 macrophages.

However, although these data prove the successful targeting of the yeast/NP complexes to macrophages, they do not reflect the real amount of delivered particles. This is mainly based on the fact that yeast/NP complexes contain only a fraction of the particle amount originally used for complexation (~38% bound NPs as determined by gradient centrifugation). To take this into account, we normalized the respective mean fluorescence intensities to the applied amount of particles actually bound to the yeast cells (Figure 6b). The resulting values make the gain in delivery efficacy by using *S. cerevisiae* cells as NP carrier even more apparent as the fluorescence intensity using hypotonic "loaded" yeast/NP complexes is up to six times higher in M1 and three times higher in M2 macrophages in comparison to the same amount of "free" NPs. Now, even the isotonic-"loaded" yeast/NP complexes are at least as effective as the "free" NPs, again with a slight bias towards M2-polarized macrophages. Visualization of particle uptake via confocal laser scanning microscopy further confirmed the FACS data, clearly underlining an effective delivery of the yeast/NP complexes into both M1 and M2 macrophages (Figure 6c). NP aggregation within the medium can be observed in the samples treated with NPs alone and has already been reported by Nafee, Schneider, Schaefer, and Lehr (2009). Interestingly, and of importance for delivery approaches, this aggregation is diminished by complexation of NPs to yeast cells and the formation of unwanted NP conglomerates is completely avoided after treatment with yeast/NP complexes (Figure 6c).

3.3.1 | Targeted delivery of yeast/NP complexes to macrophages within coculture

In the next step, we used a coculture model consisting of primary human macrophages and HeLa cells to test whether yeast/NP complexes are able to specifically target phagocytic cells and, thus, diminish the unspecific and unwanted uptake of NPs by other cell types. In this system, cocultured cells were incubated with equal amounts of NPs either as free NPs or NP/yeast complexes and the percentage of rhodamine-positive HeLa cells and macrophages was determined by flow cytometry (Figure 7). The representative dotplots shown in Figure 7a demonstrate the expected uptake of free NPs by HeLa cells and macrophages as indicated by the shift of both populations after 4 hr towards rhodamine positivity. In contrast, using NP/yeast complexes, a strong bias of the NP uptake towards macrophages could be observed. Moreover, quantification of the rhodamine-positive mammalian cells revealed that complexation with yeast not only positively affected cell targeting but also increased the NP uptake efficacy in general from 34% to 91%. Likewise, this approach yielded an acceleration of the NP uptake by the yeast vehicles: after 0.5 hr, already 78% of the macrophages were rhodamine positive compared with only 6% after incubation with free NPs (Figure 7b). Interestingly, the salt concentration seems to have an influence on the NP uptake by macrophages. While there is no observable difference with free NPs, the amount of NP-positive macrophages incubated for 0.5 hr with NP/yeast complexes prepared in hypotonic solution is significantly higher (76%) compared with the corresponding sample prepared in an isotonic milieu (40%, Figure 7c). However, this effect is compensated after 4 hr incubation. To rule out that the preparation of the yeast/NP complexes under different osmotic conditions affects the uptake of the complexes, the phagocytosis rate of macrophages was measured by flow cytometry using CFSE-stained yeast cells. This analysis resulted in more than 96% CFSE-positive macrophages already after 0.5 hr incubation time for both NaCl concentrations, thus excluding a possible negative effect of the complexation conditions (Figure S3).

4 | DISCUSSION

Macrophages possess a broad spectrum of phenotypes resulting in a variety of protective as well as pathogenic functions (Mosser & Edwards, 2008; Murray & Wynn, 2011). In particular, their involvement in chronic inflammatory diseases and tumor promotion makes this cell type a promising target for therapeutic approaches. In this respect, NPs have recently been successfully used as a carrier to MΦ in several studies, delivering for example drugs or cytokines (Amarnath Praphakar, Munusamy, Sadasivuni, & Rajan, 2016; Mantovani, Sozzani, Locati, Allavena, & Sica, 2002; Wang et al., 2017). Nonetheless, the usage of NPs strongly suffers from the lack of cell-specific targeting, possibly leading to severe off-target effects (Brown et al., 2019; Merkel et al., 2011). Yeast cells have already

FIGURE 7 Uptake of rhodamine-labeled nanoparticles (NPs) by cocultured HeLa cells and primary human macrophages (MΦ). Cocultures were incubated with either plain NPs or opsonized NP-carrying *Saccharomyces cerevisiae* for 0.5 or 4 hr. The percentage of rhodamine-positive HeLa and macrophages was determined by flow cytometry; samples taken at 0 hr served as a negative control. (a) Representative dot plots for treatment with hypotonic NPs or NP/yeast complexes are shown. (b) Quantitative analysis comparing the uptake of plain NPs (left) and NP/yeast complexes (right) in HeLa and MΦ. (c) Quantitative analysis comparing uptake of isotonic and hypotonic NPs in macrophages, either as plain NPs (left) or as NP/yeast complexes (right). The mean values ± *SEM* of two independent experiments performed in cells from different donors and measured in duplicates each are shown. *p* Values were calculated by one-way analysis of variance (***$p < .001$)

been proven to represent an effective delivery vehicle for the specific targeting of phagocytes. Consequently, a nano-in-micro carrier consisting of NP-loaded *S. cerevisiae* cells would be a promising approach to accomplish an efficient and precise targeting to MΦ (Bazan et al., 2011; Kenngott et al., 2016; Walch et al., 2011, 2012; Walch-Rückheim et al., 2016).

Therefore, in this study, the interaction between yeast cells and chitosan-coated PLGA particles was characterized. Previous studies have shown that the attractive electrostatic force between cells and NPs is not only dependent on the particle composition itself, but also on the ionic strength in the surrounding medium. Miyazaki et al. (2014) found that the NaCl content in the solution has a large impact on the adhesion of polystyrene latex NPs onto the cell surface of *S. cerevisiae*. Thus, an isotonic NaCl concentration (154 mM) was contrasted to a low NaCl environment (5 mM) in our experiments. In fact, our results show a higher interaction between yeast cells and NPs in solutions with 5 mM NaCl compared with 154 mM NaCl, for the *S. cerevisiae* strains BY4742 and S86c. Via CLSM and corresponding fluorescence intensity profiles, the internalization of NPs in the cells could be verified for high NP concentration in 5 mM NaCl, whereas the particles seem to accumulate on the cell surface at lower concentrations. These observations are in line with the findings of Lin, Brixius, Hubbuch, Thommes, and Kula (2003) that the zeta potential of yeast cells in absolute values decreases with the increase of conductivity in the solution.

Even though most of the cells of both analyzed *S. cerevisiae* strains showed an association with NPs, there was a tendency towards a higher fluorescence intensity detectable for the strain BY4742. This phenomenon can be explained by the variability in cell wall components between the analyzed strains. It has been stated by Bazan et al. (2014) that the chitin distribution in S86c is much higher compared with BY4742 (i.e. 72% vs. 37% positive cells). Furthermore, the zeta potential of BY4742 was found to be more negative compared with S86c confirming the higher attractive electrostatic force between BY4742 and positively charged NP. Examination of the effect of chitosan-coated PLGA particles on the membrane integrity of yeast cells led to the conclusion that membrane integrity of BY4742 is impaired in the concentration range between 0.03 and 1 mg/ml in 5 mM NaCl solution, but not in 154 mM NaCl. Moreover, the loss of membrane integrity goes along with reduced viability of the yeast cells when incubated with higher concentrated NPs (above 0.25 mg/ml) in a hypotonic environment. This finding is supported by the cell death of *S. cerevisiae* after incubation with positively charged PSL nanoparticles in 5 mM NaCl (Nomura et al., 2013). However, as the developed system does not depend on the viability of the yeast, the lethal effect is assumed not to play a role in the potential applications of the system (Bazan et al., 2014).

It has already been shown that the internalization of *S. cerevisiae* can be significantly increased for M2-polarized MDM by opsonization with human serum (Seif et al., 2016). This observation depends on the fact that human serum contains opsonins, like immunoglobulins and complement-derived proteins, allowing the additional recognition of coated yeast cells by Fc and complement receptors of the respective phagocytes (Underhill & Goodridge, 2012). Our results confirm an increased uptake of opsonized yeast cells in THP-1-derived M1 as well as M2 MΦ. Further, we were able to verify that preincubation with NPs does not reduce the phagocytotic efficiency of the cells. Consequently, in coculture experiments, yeast cells not only have the ability to provide targeted delivery of NPs to macrophages, but deliver a higher amount of NPs compared with NPs alone. Additionally, while plain NPs self-aggregated in the medium (Nafee et al., 2009), particles associated with yeast were internalized by M1 and M2 MΦ almost completely. As BY4742 cells show a low NP-binding capacity in isotonic environment, the decreased delivery efficiency compared with yeast incubated with NPs in 5 mM NaCl is not surprising; however, the normalized fluorescence intensity of these cells is still comparable to MΦ treated with plain NPs confirming the effectivity of the developed system.

In conclusion, our data underline the usefulness of yeast cells as a novel delivery vehicle for functionalized nanoparticles. Considering the achievements already earned by using nanoparticles for immunotherapy, the combination with yeast cells for specific targeting to APC might lead to a substantial progress in different therapeutic approaches as suggested by Amoozgar and Goldberg (2015). Beyond the cell-specific targeting and protection of the cargo, *S. cerevisiae* offers much more possibilities like modification of the cell surface improving the application via the oral route (Kenngott et al., 2016) or provoke an antitumor immune response (Liu et al., 2018). Future experiments using NPs loaded with functional molecules will reveal the full potential of yeast/NP complexes in therapeutic approaches.

ACKNOWLEDGMENTS

This project was funded, in part, by the German Research Council (DFG, KI702) and the Saarland Landesforschungsförderprogramm to FB (LFFP 1303) and AKK (LFFP 17/08).

CONFLICT OF INTERESTS

The authors declare that there are no conflict of interests.

ORCID

Ruth Kiefer http://orcid.org/0000-0001-6352-3966
Alexandra K. Kiemer http://orcid.org/0000-0002-7224-9900
Marc Schneider http://orcid.org/0000-0002-9260-7357
Frank Breinig http://orcid.org/0000-0003-1557-4691

REFERENCES

Amarnath Praphakar, R., Munusamy, M. A., Sadasivuni, K. K., & Rajan, M. (2016). Targeted delivery of rifampicin to tuberculosis-infected macrophages: Design, in-vitro, and in-vivo performance of rifampicin-loaded poly(ester amide)s nanocarriers. *International Journal of Pharmaceutics*, *513*(1-2), 628–635. https://doi.org/10.1016/j.ijpharm.2016.09.080

Amoozgar, Z., & Goldberg, M. S. (2015). Targeting myeloid cells using nanoparticles to improve cancer immunotherapy. *Advanced Drug Delivery Reviews*, *91*, 38–51. https://doi.org/10.1016/j.addr.2014.09.007

Bala, I., Hariharan, S., & Kumar, M. N. (2004). PLGA nanoparticles in drug delivery: The state of the art. *Critical Reviews in Therapeutic Drug Carrier Systems*, *21*(5), 387–422.

Bazan, S. B., Breinig, T., Schmitt, M. J., & Breinig, F. (2014). Heat treatment improves antigen-specific T cell activation after protein delivery by several but not all yeast genera. *Vaccine*, *32*(22), 2591–2598. https://doi.org/10.1016/j.vaccine.2014.03.043

Bazan, S. B., Geginat, G., Breinig, T., Schmitt, M. J., & Breinig, F. (2011). Uptake of various yeast genera by antigen-presenting cells and influence of subcellular antigen localization on the activation of ovalbumin-specific CD8 T lymphocytes. *Vaccine*, *29*(45), 8165–8173. https://doi.org/10.1016/j.vaccine.2011.07.141

Beier, R., & Gebert, A. (1998). Kinetics of particle uptake in the domes of Peyer's patches. *American Journal of Physiology*, *275*(1 Pt 1), 130–137.

Biswas, S. K., & Mantovani, A. (2010). Macrophage plasticity and interaction with lymphocyte subsets: Cancer as a paradigm. *Nature Immunology*, *11*(10), 889–896. https://doi.org/10.1038/ni.1937

Brown, S., Pistiner, J., Adjei, I. M., & Sharma, B. (2019). Nanoparticle properties for delivery to cartilage: The implications of disease state, synovial fluid, and off-target uptake. *Molecular Pharmaceutics*, *16*(2), 469–479. https://doi.org/10.1021/acs.molpharmaceut.7b00484

Dewan, M. Z., Vanpouille-Box, C., Kawashima, N., DiNapoli, S., Babb, J. S., Formenti, S. C., … Demaria, S. (2012). Synergy of topical toll-like receptor 7 agonist with radiation and low-dose cyclophosphamide in a mouse model of cutaneous breast cancer. *Clinical Cancer Research*, *18*(24), 6668–6678. https://doi.org/10.1158/1078-0432.CCR-12-0984

Dunn, G. P., Koebel, C. M., & Schreiber, R. D. (2006). Interferons, immunity and cancer immunoediting. *Nature Reviews Immunology*, *6*(11), 836–848. https://doi.org/10.1038/nri1961

Hamdy, S., Haddadi, A., Hung, R. W., & Lavasanifar, A. (2011). Targeting dendritic cells with nano-particulate PLGA cancer vaccine formulations. *Advanced Drug Delivery Reviews*, *63*(10-11), 943–955. https://doi.org/10.1016/j.addr.2011.05.021

Hoppstädter, J., Seif, M., Dembek, A., Cavelius, C., Huwer, H., Kraegeloh, A., & Kiemer, A. K. (2015). M2 polarization enhances silica nanoparticle uptake by macrophages. *Frontiers in Pharmacology*, *6*, 55. https://doi.org/10.3389/fphar.2015.00055

Jain, S., Tran, T. H., & Amiji, M. (2015). Macrophage repolarization with targeted alginate nanoparticles containing IL-10 plasmid DNA for the treatment of experimental arthritis. *Biomaterials*, *61*, 162–177. https://doi.org/10.1016/j.biomaterials.2015.05.028

Kenngott, E. E., Kiefer, R., Schneider-Daum, N., Hamann, A., Schneider, M., Schmitt, M. J., & Breinig, F. (2016). Surface-modified yeast cells: A novel eukaryotic carrier for oral application. *Journal of Controlled Release*, *224*, 1–7. https://doi.org/10.1016/j.jconrel.2015.12.054

Kiemer, A. K., Senaratne, R. H., Hoppstadter, J., Diesel, B., Riley, L. W., Tabeta, K., … Zuraw, B. L. (2009). Attenuated activation of macrophage TLR9 by DNA from virulent mycobacteria. *Journal of Innate Immunity*, *1*(1), 29–45. https://doi.org/10.1159/000142731

Lababidi, N., Sigal, V., Koenneke, A., Schwarzkopf, K., Manz, A., & Schneider, M. (2019). Microfluidics as tool to prepare size-tunable PLGA nanoparticles with high curcumin encapsulation for efficient mucus penetration. *Beilstein Journal of Nanotechnology*, *10*, 2280–2293. https://doi.org/10.3762/bjnano.10.220

Lin, D. Q., Brixius, P. J., Hubbuch, J. J., Thommes, J., & Kula, M. R. (2003). Biomass/adsorbent electrostatic interactions in expanded bed adsorption: A zeta potential study. *Biotechnology and Bioengineering*, *83*(2), 149–157. https://doi.org/10.1002/bit.10654

Liu, D. Q., Lu, S., Zhang, L. X., Ji, M., Liu, S. Y., Wang, S. W., & Liu, R. T. (2018). An indoleamine 2, 3-dioxygenase siRNA nanoparticle-coated and Trp2-displayed recombinant yeast vaccine inhibits melanoma tumor growth in mice. *Journal of Controlled Release*, *273*, 1–12. https://doi.org/10.1016/j.jconrel.2018.01.013

Mantovani, A., Sozzani, S., Locati, M., Allavena, P., & Sica, A. (2002). Macrophage polarization: Tumor-associated macrophages as a paradigm for polarized M2 mononuclear phagocytes. *Trends in Immunology*, *23*(11), 549–555.

Merkel, O. M., Beyerle, A., Beckmann, B. M., Zheng, M., Hartmann, R. K., Stoger, T., & Kissel, T. H. (2011). Polymer-related off-target effects in non-viral siRNA delivery. *Biomaterials*, *32*(9), 2388–2398. https://doi.org/10.1016/j.biomaterials.2010.11.081

Mir, M., Ahmed, N., & Rehman, A. U. (2017). Recent applications of PLGA based nanostructures in drug delivery. *Colloids and Surfaces B: Biointerfaces*, *159*, 217–231. https://doi.org/10.1016/j.colsurfb.2017.07.038

Miyazaki, J., Kuriyama, Y., Miyamoto, A., Tokumoto, H., Konishi, Y., & Nomura, T. (2014). Adhesion and internalization of functionalized polystyrene latexnanoparticles toward the yeast *Saccharomyces cerevisiae*. *Advanced Powder Technology*, *25*, 1394–1397.

Mosser, D. M., & Edwards, J. P. (2008). Exploring the full spectrum of macrophage activation. *Nature Reviews Immunology*, *8*(12), 958–969. https://doi.org/10.1038/nri2448

Murray, P. J., & Wynn, T. A. (2011). Protective and pathogenic functions of macrophage subsets. *Nature Reviews Immunology*, *11*(11), 723–737. https://doi.org/10.1038/nri3073

Nafee, N., Schneider, M., Schaefer, U. F., & Lehr, C. M. (2009). Relevance of the colloidal stability of chitosan/PLGA nanoparticles on their cytotoxicity profile. *International Journal of Pharmaceutics*, *381*(2), 130–139. https://doi.org/10.1016/j.ijpharm.2009.04.049

Nafee, N., Taetz, S., Schneider, M., Schaefer, U. F., & Lehr, C. M. (2007). Chitosan-coated PLGA nanoparticles for DNA/RNA delivery: Effect of the formulation parameters on complexation and transfection of antisense oligonucleotides. *Nanomedicine: Nanotechnology, Biology and Medicine*, *3*(3), 173–183. https://doi.org/10.1016/j.nano.2007.03.006

Nomura, T., Miyazaki, J., Miyamoto, A., Kuriyama, Y., Tokumoto, H., & Konishi, Y. (2013). Exposure of the yeast *Saccharomyces cerevisiae* to functionalized polystyrene latex nanoparticles: Influence of surface charge on toxicity. *Environmental Science and Technology*, *47*(7), 3417–3423. https://doi.org/10.1021/es400053x

Reinartz, S., Schumann, T., Finkernagel, F., Wortmann, A., Jansen, J. M., Meissner, W., … Muller, R. (2014). Mixed-polarization phenotype of ascites-associated macrophages in human ovarian carcinoma: Correlation of CD163 expression, cytokine levels and early relapse. *International Journal of Cancer*, *134*(1), 32–42. https://doi.org/10.1002/ijc.28335

Ren, T., Gou, J., Sun, W., Tao, X., Tan, X., Wang, P., … Tang, X. (2018). Entrapping of nanoparticles in yeast cell wall microparticles for macrophage-targeted oral delivery of cabazitaxel. *Molecular Pharmaceutics*, *15*(7), 2870–2882. https://doi.org/10.1021/acs.molpharmaceut.8b00357

Rubio, C., Munera-Maravilla, E., Lodewijk, I., Suarez-Cabrera, C., Karaivanova, V., Ruiz-Palomares, R., … Duenas, M. (2019). Macrophage polarization as a novel weapon in conditioning tumor microenvironment for bladder cancer: Can we turn demons into gods? *Clinical and Translational Oncology*, *21*(4), 391–403. https://doi.org/10.1007/s12094-018-1952-y

Seif, M., Hoppstädter, J., Breinig, F., & Kiemer, A. K. (2017). Yeast-mediated mRNA delivery polarizes immuno-suppressive macrophages towards an immuno-stimulatory phenotype. *European Journal of Pharmaceutics and Biopharmaceutics*, *117*, 1–13. https://doi.org/10.1016/j.ejpb.2017.03.008

Seif, M., Philippi, A., Breinig, F., Kiemer, A. K., & Hoppstädter, J. (2016). Yeast (*Saccharomyces cerevisiae*) polarizes both M-CSF- and GM-CSF-differentiated macrophages toward an M1-like phenotype. *Inflammation*, *39*(5), 1690–1703. https://doi.org/10.1007/s10753-016-0404-5

Soto, E. R., Caras, A. C., Kut, L. C., Castle, M. K., & Ostroff, G. R. (2012). Glucan particles for macrophage targeted delivery of nanoparticles. *Journal of Drug Delivery*, *2012*(2012), 1–13. https://doi.org/10.1155/2012/143524

Soto, E. R., & Ostroff, G. R. (2008). Characterization of multilayered nanoparticles encapsulated in yeast cell wall particles for DNA delivery. *Bioconjugate Chemistry*, *19*(4), 840–848. https://doi.org/10.1021/bc700329p

Stubbs, A. C., Martin, K. S., Coeshott, C., Skaates, S. V., Kuritzkes, D. R., Bellgrau, D., … Wilson, C. C. (2001). Whole recombinant yeast vaccine activates dendritic cells and elicits protective cell-mediated immunity. *Nature Medicine*, *7*(5), 625–629.

Underhill, D. M., & Goodridge, H. S. (2012). Information processing during phagocytosis. *Nature Reviews Immunology*, *12*(7), 492–502. https://doi.org/10.1038/nri3244

Verreck, F. A., de Boer, T., Langenberg, D. M., van der Zanden, L., & Ottenhoff, T. H. (2006). Phenotypic and functional profiling of human proinflammatory type-1 and anti-inflammatory type-2 macrophages in response to microbial antigens and IFN-γ- and CD40L-mediated costimulation. *Journal of Leukocyte Biology*, *79*(2), 285–293. https://doi.org/10.1189/jlb.0105015

Walch-Rückheim, B., Kiefer, R., Geginat, G., Schmitt, M. J., & Breinig, F. (2016). Coexpression of human perforin improves yeast-mediated delivery of DNA and mRNA to mammalian antigen-presenting cells. *Gene Therapy*, *23*(1), 103–107. https://doi.org/10.1038/gt.2015.77

Walch, B., Breinig, T., Geginat, G., Schmitt, M. J., & Breinig, F. (2011). Yeast-based protein delivery to mammalian phagocytic cells is increased by coexpression of bacterial listeriolysin. *Microbes and Infection*, *13*(11), 908–913. https://doi.org/10.1016/j.micinf.2011.05.006

Walch, B., Breinig, T., Schmitt, M. J., & Breinig, F. (2012). Delivery of functional DNA and messenger RNA to mammalian phagocytic cells by recombinant yeast. *Gene Therapy*, *19*(3), 237–245. https://doi.org/10.1038/gt.2011.121

Wang, Y., Lin, Y. X., Qiao, S. L., An, H. W., Ma, Y., Qiao, Z. Y., … Wang, H. (2017). Polymeric nanoparticles promote macrophage reversal from M2 to M1 phenotypes in the tumor microenvironment. *Biomaterials*, *112*, 153–163. https://doi.org/10.1016/j.biomaterials.2016.09.034

Xue, J., Schmidt, S. V., Sander, J., Draffehn, A., Krebs, W., Quester, I., … Schultze, J. L. (2014). Transcriptome-based network analysis reveals a spectrum model of human macrophage activation. *Immunity*, *40*(2), 274–288. https://doi.org/10.1016/j.immuni.2014.01.006

Zhou, X., Zhang, X., Han, S., Dou, Y., Liu, M., Zhang, L., … Zhang, J. (2017). Yeast microcapsule-mediated targeted delivery of diverse nanoparticles for imaging and therapy via the oral route. *Nano Letters*, *17*(2), 1056–1064. https://doi.org/10.1021/acs.nanolett.6b04523

SUPPORTING INFORMATION

Additional supporting information may be found online in the Supporting Information section.

How to cite this article: Kiefer R, Jurisic M, Dahlem C, et al. Targeted delivery of functionalized PLGA nanoparticles to macrophages by complexation with the yeast *Saccharomyces cerevisiae*. *Biotechnology and Bioengineering*. 2020;117:776–788. https://doi.org/10.1002/bit.27226